

Supporting Information for:

Optimization of the carbon to nitrogen ratio for mainstream deammonification and the resulting shift in nitrification from biofilm to suspension

Paul Roots, Alex Rosenthal, Quan Yuan, Yubo Wang, Fenghua Yang, Heng Zhang, Joseph Kozak, George Wells

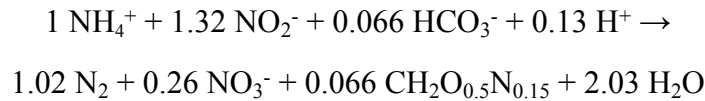
Supporting Information contains 10 pages with 7 Figures

Batch Activity Assays

In situ Maximum Anammox Activity Assays

Anammox maximum activity tests were performed *in situ* at the end of reactor cycles when sCOD was low to minimize interference from denitrifiers. NH_4^+ and NO_2^- were spiked to non-limiting conditions (20 – 40 mgN/L each) via ammonium chloride and sodium nitrite salt solutions and the reactor was mixed without aeration. To prevent oxygen intrusion, around day 540 several 1.4-inch diameter floating spheres (similar to ping pong balls) were added to cover the surface of the reactor and were left in place until end of the study. N_2 gas sparging was performed during the tests on days 800 and 867 but was not continued due to pH increase (from CO_2 sparging) and the lack of a discernable difference in activity. Five to six grab samples were taken in 30-minute intervals and analyzed for NH_4^+ , NO_2^- and NO_3^- by colorimetry.¹

According to stoichiometry from Strous et al. (1998),² the anammox metabolic pathway removes N (as nitrogen gas + biomass) at a ratio of 2.05 moles N per mole NH_4^+ removed:



Anammox activity as N removal (in mg N/L/d) was therefore calculated as 2.05 times the slope of the NH_4^+ drawdown curve. Only linear trends with R^2 values above 0.8 were used. Stoichiometric ratios of NO_2^- drawdown and NO_3^- production to NH_4^+ drawdown were compared to anammox stoichiometry to check that anammox was the dominant metabolic pathway. Higher than expected NO_2^- drawdown and lower than expected NO_3^- production occasionally indicated the presence of denitrification in these tests, by which we inferred that use of the NH_4^+ drawdown curve alone (with anammox stoichiometry) was the most accurate method for calculating anammox activity.

Ex situ Maximum AOB and NOB Activity Assays

AOB and NOB maximum activity assays were performed separately for carrier and suspended biomass (both in duplicate) via *ex situ* assays. For suspended biomass, 300 mL of mixed liquor from the end of a react cycle (to minimize sCOD concentration and interference from denitrifiers) was placed into each of two 500-mL Erlenmeyer flasks. For carrier biomass activity, K5 carriers were counted and placed into a final volume of 300 mL of reactor effluent in each of two 500-mL Erlenmeyer flasks to match the volumetric carrier filling ratio of the reactor (30 – 38% depending on date). The four flasks were placed on a shaker table with a water bath for temperature control between 10 – 22 °C to match the reactor temperature at the time. DO was monitored with a Hach LDO® optical DO probe and was maintained at or above 3 mgO₂/L by shaking action and bubbling from small aquarium pumps. pH was monitored with the Hach PHC101® electrode and maintained between 7 and 8. NH_4^+ and NO_2^- were spiked to non-limiting conditions (~20 mg NH_4^+ -N/L and ~10 mg NO_2^- -N/L), and five grab samples were taken in 20-minute intervals and analyzed for NH_4^+ , NO_2^- and NO_3^- by colorimetry (APHA, 2005). AOB activity was taken as the slope of the NH_4^+ drawdown curve, and NOB was taken as the average of the (1) slope of the NO_3^- production curve and (2) the sum of the slopes of NH_4^+ and

NO_2^- drawdown curves. Only linear trends with R^2 values above 0.8 were used. In some carrier tests (likely due to the presence of anoxic zones in the biofilm), a decline in TIN (i.e. $\text{NH}_4^+ + \text{NO}_2^- + \text{NO}_3^-$ linear fit with $R^2 > 0.8$) over the course of the test indicated the presence of anammox activity, and AOB and NOB activities were adjusted accordingly via the anammox stoichiometry shown above.

Nitrogen Isotope Testing

Nitrogen stable isotope testing was performed on days 1,100, 1,112 and 1,128 to estimate the relative contributions of anammox and denitrification to N removal following Wang et al. (2015).³ Isotopes of $^{15}\text{NH}_4^+$, $^{15}\text{NO}_3^-$ and $^{15}\text{NO}_2^-$ were spiked separately under initially anaerobic conditions (i.e. with no O_2 , $^{14}\text{NO}_3^-$, or $^{14}\text{NO}_2^-$ present), with $^{14}\text{NH}_4^+$ already present in solution, to quantify the percent contribution of anammox and denitrification by measuring the relative amounts of $^{29}\text{N}_2$ and $^{30}\text{N}_2$ produced, respectively. In this test, the anammox metabolic pathway produces $^{29}\text{N}_2$ by combining one molecule of $^{14}\text{NH}_4^+$ and one molecule of $^{15}\text{NO}_2^-$, while the denitrification metabolic pathway produces $^{30}\text{N}_2$ by combining two molecules of $^{15}\text{NO}_2^-$ and/or $^{15}\text{NO}_3^-$. The $^{15}\text{NH}_4^+$ -spiked test was used as a control to ensure anaerobic conditions (i.e. the absence of $^{14}\text{NO}_3^-$ and $^{14}\text{NO}_2^-$) such that minimal $^{29}\text{N}_2$ and $^{30}\text{N}_2$ production should be observed. A blank vial, with no ^{15}N chemical spiked but all other conditions the same, was also included. Aside from the lack of aeration during isotope testing, test conditions were prepared to mimic in-cycle conditions as closely as possible. Carrier and suspended biomass were collected together in 250-mL vials in the middle of a typical cycle to mimic average organic carbon availability. Before spiking, the test vials were bubbled with Helium gas, capped, and shaken for 9 hours to ensure reduction of residual O_2 and $^{14}\text{NO}_X^-$ ($^{14}\text{NO}_3^- + ^{14}\text{NO}_2^-$). 10 mgN/L of $^{14}\text{NH}_4^+$ was chosen as a typical in-cycle NH_4^+ concentration, and 7 mgN/L of $^{15}\text{NH}_4^+$, $^{15}\text{NO}_3^-$ or $^{15}\text{NO}_2^-$ was spiked to separate bottles in duplicate to ensure that anammox would not become NH_4^+ -limited during the test. After spiking ^{15}N chemicals the vials were shaken for > 14 hours at room temperature (23 °C).

Mass spectrometry of the N_2 isotopologues, in order to determine the relative abundance of $^{28,29,30}\text{N}_2$, was performed immediately after sub-sampling the vials with a 100- μL gas-tight (Hamilton) syringe. Samples were withdrawn from the vials, immediately injected into a UHP He purged and septum sealed 12-mL Exetainer, and transferred to a thermo-stated (30 °C) incubation block of a GasBench II. Exetainers were sub-sampled further with the a double bore needle of a PAL autosampler, and loaded-injected into the GasBench II via a 100- μL injection loop at a flow-rate of 1.2 mL/min, dried 2X in a Nafion drier, and separated on a GC column (0.18 mm ID) held at 70 °C. The open-split of the GasBench II was further mated to a Thermo Delta V Plus isotope ratio mass-spectrometer, run in continuous flow mode (Thermo Scientific™, Waltham MA, USA), outfitted with three Faraday cup collectors (3×10^8 , 3×10^{10} , 1×10^{11} ohms). Pure N_2 gas (containing 99.634% of ^{14}N and 0.366% of ^{15}N typical of atmospheric N_2) was used for calibration of $^{28,29,30}\text{N}_2$ (via independent collectors) with 5 injection volumes from 20 and 100 μL . 40 μL of gas was extracted from the headspace of each test vial for analysis; this volume was chosen to ensure that signal intensity remained well within the linear range (200 mV – 20 V) of the instrument and to avoid memory effects between samples. The quantity in mmol of each of $^{28,29,30}\text{N}_2$ for each sample injection was calculated from the calibration curve. The quantity in mmol of each of $^{28,29,30}\text{N}_2$ in the vial headspace was then inferred by multiplying by the ratio of the vial headspace volume to the injection volume (average multiplying factor = 795).

The $^{29}\text{N}_2$ and $^{30}\text{N}_2$ produced for each sample was defined as the difference between the mmol of $^{29}\text{N}_2$ or $^{30}\text{N}_2$ in each sample vial headspace and the $^{29}\text{N}_2$ or $^{30}\text{N}_2$ in the blank vial headspace.

Biomass sampling

Suspended (floccular) and carrier (biofilm) biomass was sampled once or twice per month for 16S rRNA gene sequencing analyses. For the suspended biomass, four 1-mL aliquots of mixed liquor were centrifuged at 10,000g for 3 minutes, and the supernatant was replaced with 1 mL of Tris-EDTA buffer. The biomass pellet was then vortexed and centrifuged at 10,000g for 3 minutes after which the supernatant was removed, leaving only the biomass pellet to be archived at $-80\text{ }^\circ\text{C}$. For the carrier biomass whole K5 biocarriers were sampled and archived directly at $-80\text{ }^\circ\text{C}$. Biofilm was scraped off a 1/8th section of the archived K5 biocarriers immediately before performing DNA extraction.

16S rRNA Gene Sequencing

16S rRNA gene amplicon library preparations were performed using a two-step PCR protocol using the Fluidigm Biomark: Multiplex PCR Strategy as previously described.⁴ In the first round of PCR, each 20 μL reaction contained 10 μL of FailSafe PCR 2X PreMix F (Epicentre, Madison, WI), 0.63 units of Expand High Fidelity PCR Taq Enzyme (Sigma-Aldrich, St. Louis, MO), 0.4 μM of forward primer and reverse primer modified with Fluidigm common sequences at the 5' end of each primer, 1 μL of gDNA (approximately 100 ng) and the remaining volume molecular biology grade water. The V4-V5 region of the 16S rRNA gene was amplified using the 515F-Y (5'-GTGYCAGCMGCCGCGGTAA-3') and 926R (5'-CCGYCAATTYMTTTRAGTTT-3') primer set.⁵ PCR reactions were run with a Biorad T-100 Thermocycler (Bio-Rad, Hercules, CA). Thermocycling conditions for the 515F-Y/926R primer set were 95°C for 5 minutes, then 28 cycles of 95°C for 30 seconds, 50°C for 45 seconds, and 68°C for 30 seconds, followed by a final extension of 68°C for 5 minutes. Specificity of amplification was checked for all samples via agarose gel electrophoresis.

Sample barcoding (i.e. second-stage PCR) and sequencing was performed at the University of Illinois at Chicago DNA Services Facility. Sequencing was done on an Illumina MiSeq sequencer (Illumina, San Diego, CA) using Illumina V2 (2x250 paired end) chemistry. For amplicon sequence analysis, sequence quality control was performed through DADA2⁶ integrated in QIIME2 version qiime2-2018.8,⁷ which included quality-score-based sequence truncation, primer trimming, merging of paired-end reads, and removal of chimeras. Taxonomy was assigned to each individual sequence variation using the Silva database, release 132.

qPCR

qPCR reactions were run on a Bio-Rad C1000 CFX96 Real-Time PCR system (Bio-Rad, Hercules, CA, USA). Each sample date included 2 technical replicates of 2 biological replicates (total of 4 replicates), and the standard series was generated in duplicate on each plate by tenfold serial dilutions of synthesized DNA (IDT Inc, Coralville, IA, USA). 20 μL reactions included 10 μL of the Bio-Rad SsoAdvanced Universal Inhibitor-Tolerant SYBR Green Supermix (Bio-Rad, Hercules, CA, USA), 0.5 μM of each primer, 1 μL of standard or 10-fold diluted DNA extracts, and the balance molecular biology grade water. Amplification specificity was verified for all samples via melt curve analysis, and for select samples via gel electrophoresis.

Supplementary Figures

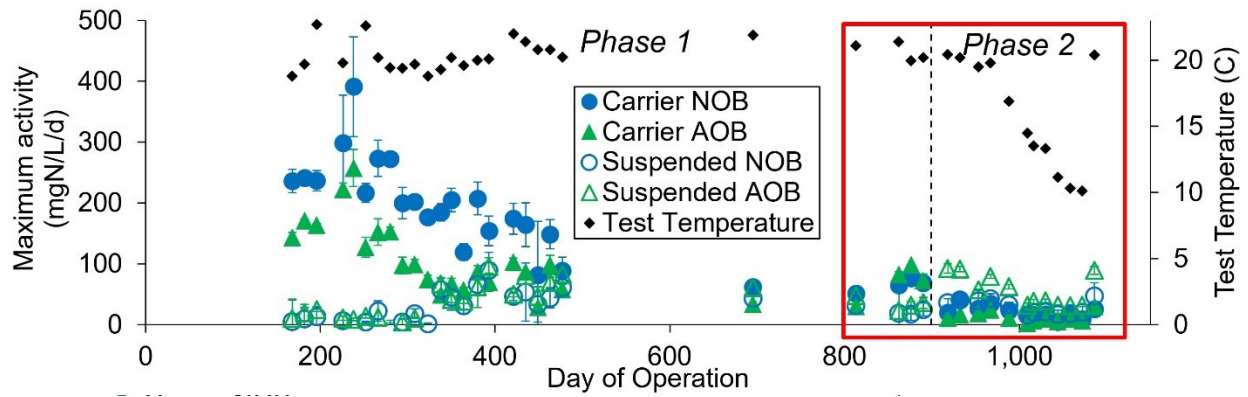


Figure S1. Maximum AOB and NOB activities in the suspended biomass and on the carriers as measured in *ex situ* batch activity assays over the entire project. The red box outlines the data shown in Figure 4.

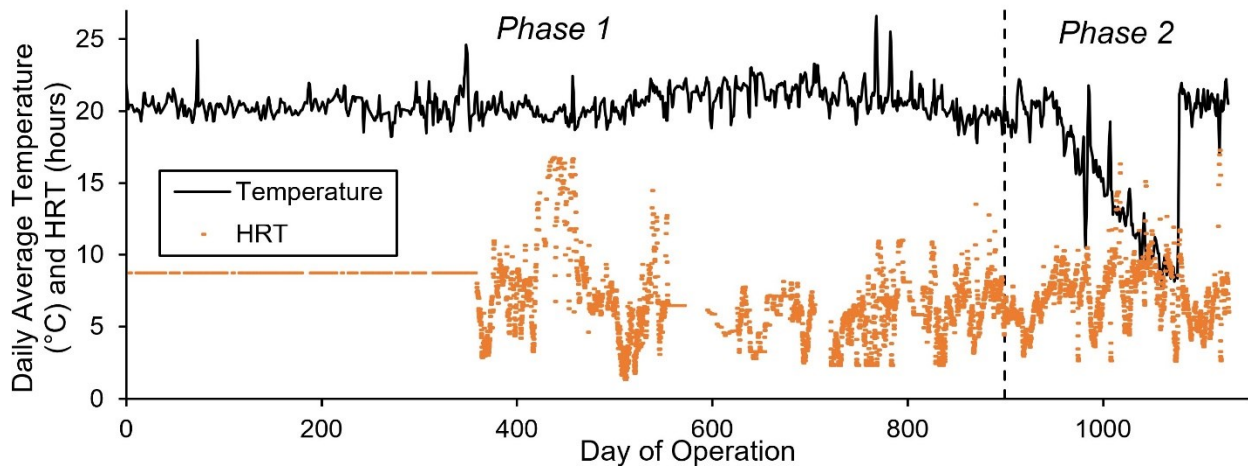


Figure S2. Hydraulic retention time (HRT) and daily average reactor temperature throughout the study. Variable HRT began on day 358 upon implementation of ammonia-based control, whereupon the aerated portion of the cycle was terminated when the target effluent ammonia concentration of 2 mg $\text{NH}_4^+\text{-N/L}$ was reached. After day 358 the HRT was calculated on a per-cycle basis.

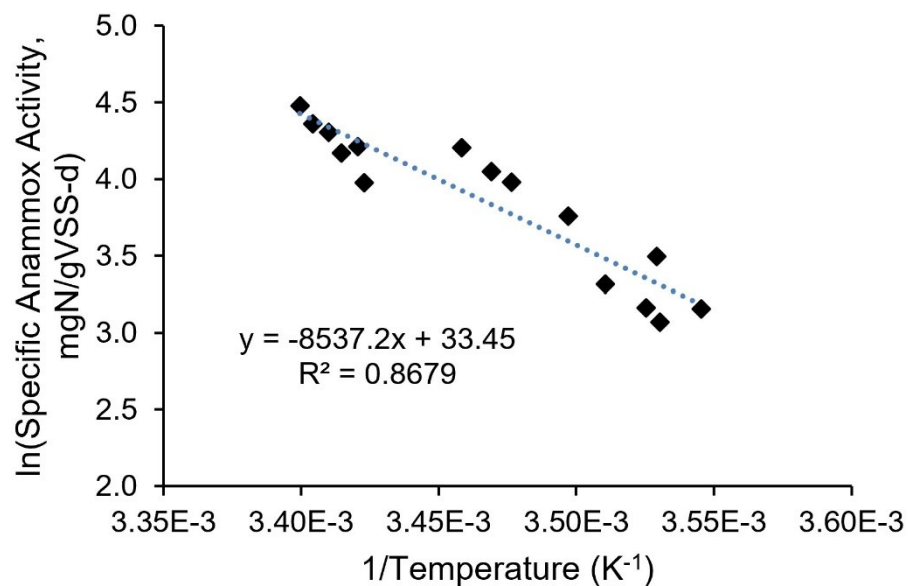


Figure S3. Arrhenius plot of 15 maximum specific anammox activity tests (normalized to total carrier biomass) during Phase 2 (days 904 – 1,121). The activation energy calculated from the slope was 71 ± 8 kJ/mol (\pm standard error of the slope), though this should not be interpreted as a strict activation energy considering possible temperature adaptation and shifts in the microbial community over the 217 days.

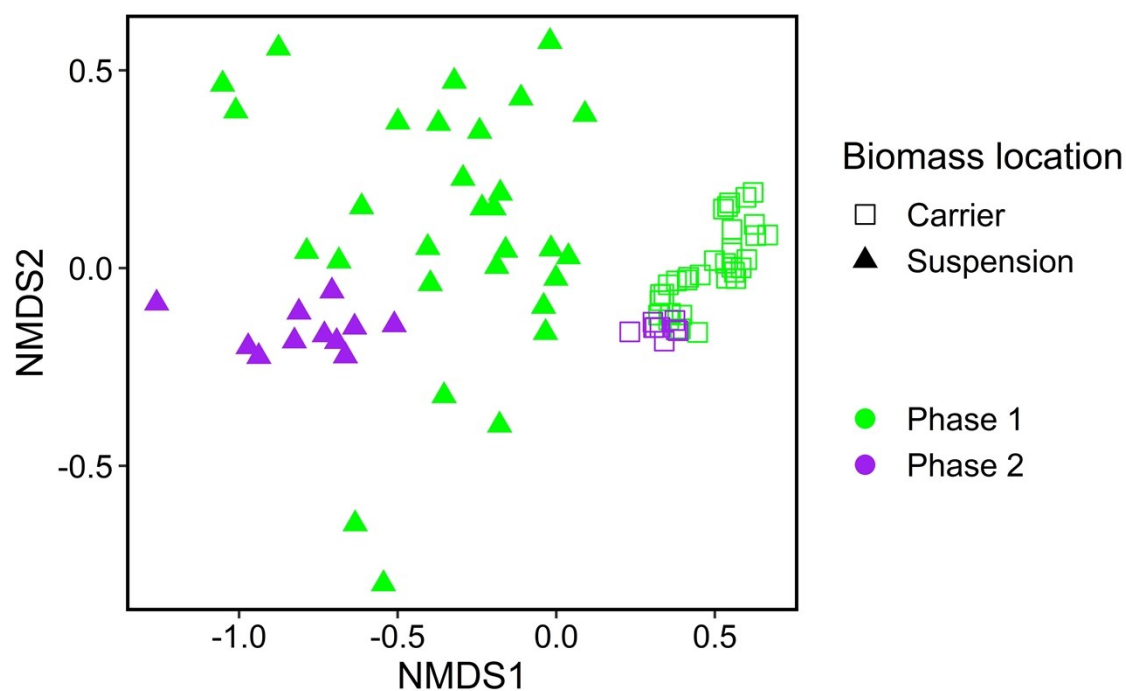


Figure S4: Non-metric multidimensional scaling (NMDS) ordination of all carrier and suspended biomass samples as calculated from genus-level 16S rRNA gene sequencing data. In

order to facilitate convergence of the solution, the data was first trimmed to remove the least abundant genera comprising 0.09% of the total abundance. The significance of the ordination is represented by the stress value of 0.096.

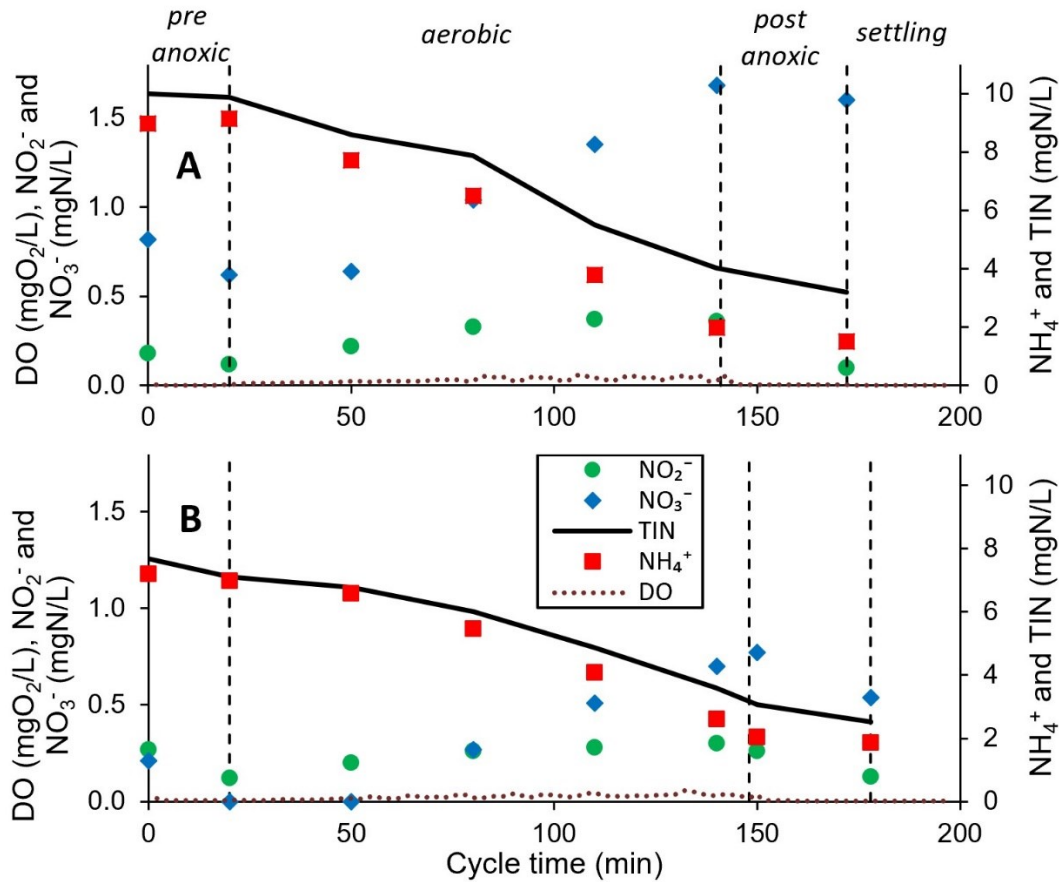


Figure S5. Two representative in-cycle tests during Phase 2 from (A) day 909 at 18.9 °C and (B) day 1107 at 21.1 °C. Reactor fill (not shown) occurred in less than 2 minutes, and cycle time = 0 is defined as the completion of fill.

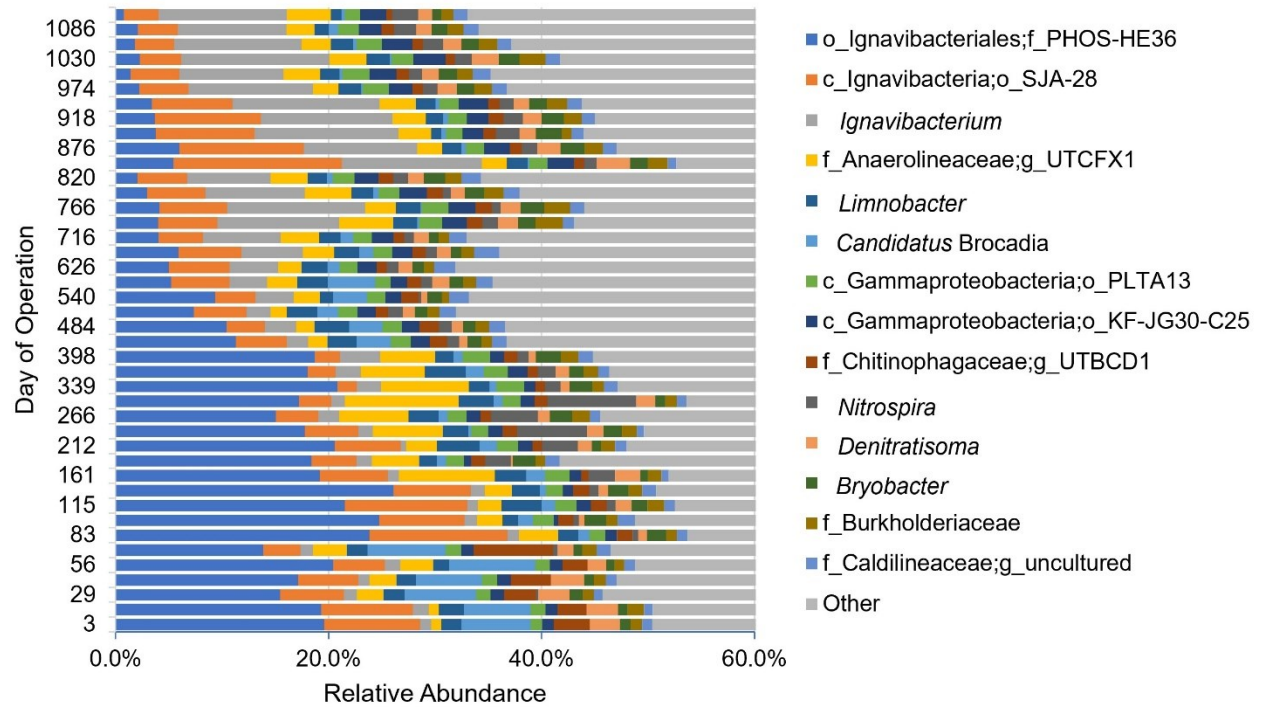


Figure S6. Relative abundance of the 14 most abundant bacterial genera in the carrier biomass according to 16S rRNA gene sequencing. Amplicon sequence variants that were unclassified at the genus level are presented with the corresponding lowest annotable taxonomy: p_ = phylum, c_ = class, o_ = order, f_ = family, g_ = genus.

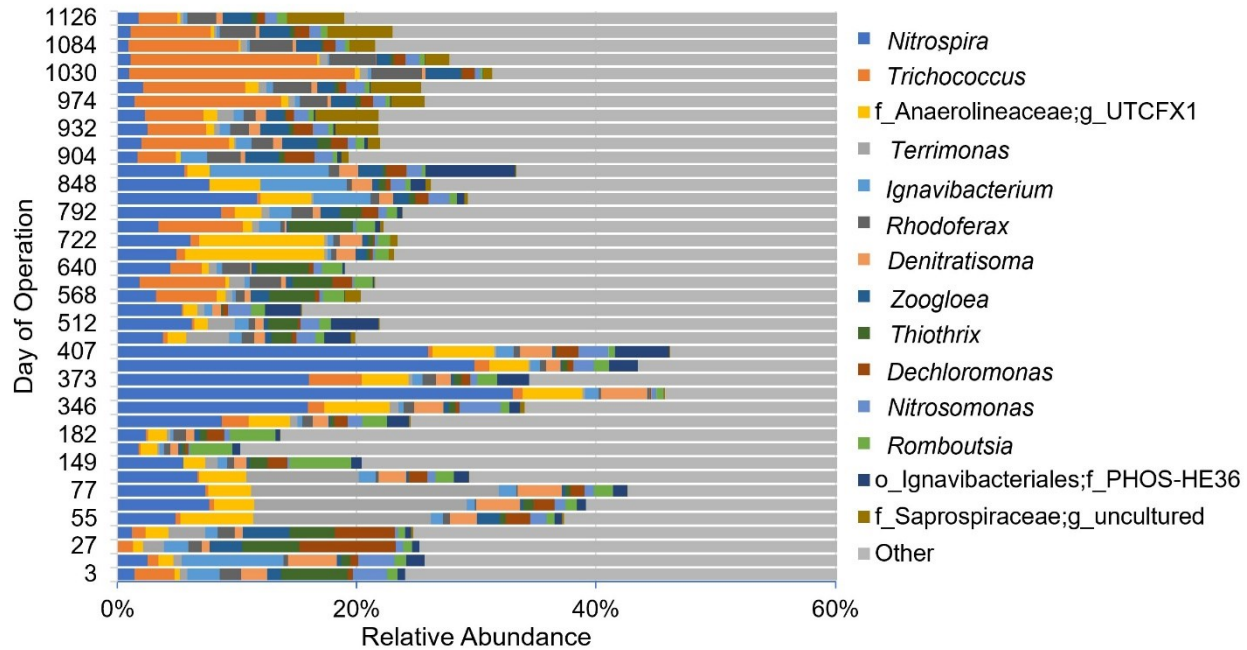


Figure S7. Relative abundance of the 14 most abundant bacterial genera in the suspended biomass according to 16S rRNA gene sequencing. Amplicon sequence variants that were unclassified at the genus level are presented with the corresponding lowest annotable taxonomy: o_ = order, f_ = family, g_ = genus.

References for Supporting Information

- (1) APHA. *Standard Methods for the Examination of Water and Wastewater*, 21st ed.; American Public Health Association: Washington, D.C., 2005.
- (2) Strous, M.; Heijnen, J. J.; Kuenen, J. G.; Jetten, M. S. M. The Sequencing Batch Reactor as a Powerful Tool for the Study of Slowly Growing Anaerobic Ammonium-Oxidizing Microorganisms. *Appl. Microbiol. Biotechnol.* **1998**, *50* (5), 589–596.
- (3) Wang, S.; Peng, Y.; Ma, B.; Wang, S.; Zhu, G. Anaerobic Ammonium Oxidation in Traditional Municipal Wastewater Treatment Plants with Low-Strength Ammonium Loading: Widespread but Overlooked. *Water Res.* **2015**, *84*, 66–75. <https://doi.org/10.1016/j.watres.2015.07.005>.
- (4) Griffin, J. S.; Wells, G. F. Regional Synchrony in Full-Scale Activated Sludge Bioreactors Due to Deterministic Microbial Community Assembly. *ISME J.* **2017**, *11* (2), 500–511. <https://doi.org/10.1038/ismej.2016.121>.
- (5) Parada, A. E.; Needham, D. M.; Fuhrman, J. A. Every Base Matters: Assessing Small Subunit RRNA Primers for Marine Microbiomes with Mock Communities, Time Series and Global Field Samples: Primers for Marine Microbiome Studies. *Environ. Microbiol.* **2016**, *18* (5), 1403–1414. <https://doi.org/10.1111/1462-2920.13023>.

- (6) Callahan, B. J.; McMurdie, P. J.; Rosen, M. J.; Han, A. W.; Johnson, A. J. A.; Holmes, S. P. DADA2: High-Resolution Sample Inference from Illumina Amplicon Data. *Nat. Methods* **2016**, *13* (7), 581–583. <https://doi.org/10.1038/nmeth.3869>.
- (7) Bolyen, E.; Rideout, J. R.; Dillon, M. R.; Bokulich, N. A.; Abnet, C.; Al-Ghalith, G. A.; Alexander, H.; Alm, E. J.; Arumugam, M.; Asnicar, F.; Bai, Y.; Bisanz, J. E.; Bittinger, K.; Brejnrod, A.; Brislawn, C. J.; Brown, C. T.; Callahan, B. J.; Caraballo-Rodríguez, A. M.; Chase, J.; Cope, E.; Da Silva, R.; Dorrestein, P. C.; Douglas, G. M.; Durall, D. M.; Duvallet, C.; Edwardson, C. F.; Ernst, M.; Estaki, M.; Fouquier, J.; Gauglitz, J. M.; Gibson, D. L.; Gonzalez, A.; Gorlick, K.; Guo, J.; Hillmann, B.; Holmes, S.; Holste, H.; Huttenhower, C.; Huttley, G.; Janssen, S.; Jarmusch, A. K.; Jiang, L.; Kaehler, B.; Kang, K. B.; Keefe, C. R.; Keim, P.; Kelley, S. T.; Knights, D.; Koester, I.; Kosciulek, T.; Kreps, J.; Langille, M. G.; Lee, J.; Ley, R.; Liu, Y.-X.; Loftfield, E.; Lozupone, C.; Maher, M.; Marotz, C.; Martin, B.; McDonald, D.; McIver, L. J.; Melnik, A. V.; Metcalf, J. L.; Morgan, S. C.; Morton, J.; Naimey, A. T.; Navas-Molina, J. A.; Nothias, L. F.; Orchanian, S. B.; Pearson, T.; Peoples, S. L.; Petras, D.; Preuss, M. L.; Pruesse, E.; Rasmussen, L. B.; Rivers, A.; Robeson, II, M. S.; Rosenthal, P.; Segata, N.; Shaffer, M.; Shiffer, A.; Sinha, R.; Song, S. J.; Spear, J. R.; Swafford, A. D.; Thompson, L. R.; Torres, P. J.; Trinh, P.; Tripathi, A.; Turnbaugh, P. J.; Ul-Hasan, S.; van der Hooft, J. J.; Vargas, F.; Vázquez-Baeza, Y.; Vogtmann, E.; von Hippel, M.; Walters, W.; Wan, Y.; Wang, M.; Warren, J.; Weber, K. C.; Williamson, C. H.; Willis, A. D.; Xu, Z. Z.; Zaneveld, J. R.; Zhang, Y.; Knight, R.; Caporaso, J. G. QIIME 2: Reproducible, Interactive, Scalable, and Extensible Microbiome Data Science. *PeerJ* **2018**. <https://doi.org/10.7287/peerj.preprints.27295v1>.